JEE Journal of Ecological Engineering

Journal of Ecological Engineering, 2026, 27(7), 148–164
https://doi.org/10.12911/22998993/218555
ISSN 2299–8993, License CC-BY 4.0

Received: 2026.01.29
Accepted: 2026.05.20
Published: 2026.06.01

Annual temperature and moisture dynamics of a Mollisol profile under a soybean-maize cropping system

Yuriy Kravchenko[1*], Xingyi Zhang[2], Volodymyr Voitsekhivskyi[1], Olena Voitsekhivska[3], Vasyl Vakhnyak[4], Halyna Yakivna Slobodianyk[5], Vasyl Krasnoshtan[5]

[1] National University of Life and Environmental Sciences of Ukraine, 15 Heroyiv Oborony St., 03041, Kyiv, Ukraine
[2] Northeast Institute of Geography and Agroecology, 138 Harping Rd, 150081, Harbin, China
[3] Taras Shevchenko National University of Kyiv, Institute of Biology and Medicine, 64/13 Volodymyrska St., 01601, Kyiv, Ukraine
[4] Higher educational institution "Podillia State University", 12 Shevchenko St., 32316, Kamianets-Podilskyi, Ukraine
[5] Uman National University, 2 Sadova St., 20300, Uman, Ukraine
* Corresponding author's e-mail: kravch@nubip.edu.ua

ABSTRACT

Soil temperature and moisture jointly regulate agronomic processes; however, their coupled dynamics across the entire soil profile remain insufficiently resolved under contrasting tillage systems. This study investigated the annual hydrothermal dynamics of a Mollisol under a soybean–maize rotation managed with conventional (CT), reduced (RT), and no-till (NT) practices in Northeast China. High-resolution automated monitoring from 5 to 270 cm over multiple years revealed that tillage established two distinct pedophysical regimes. No-till functioned as a capacitively buffered system characterized by high structural inertia. NT exhibited a 33% slower autumn cooling rate, a 108% longer winter near-isothermal period indicative of prolonged latent heat release, and a 47% slower spring warming rate at the surface compared with CT. Concurrently, CT exhibited significantly lower volumetric water content (θ_v) throughout most of the year. During peak summer deficit, surface θ_v under NT was 49% higher than under CT. In contrast, CT operated as a conductive–advective regime, displaying rapid thermal responses, deeper frost penetration, and episodic winter warming pulses associated with advective heat transfer via upward water migration, which depleted deep soil moisture reserves. These findings reveal a critical agronomic trade-off: CT provided a warmer seedbed in spring (accumulating 55 additional growing degree days >5 °C by late May), whereas NT ensured superior moisture retention during climatically sensitive reproductive stages. Conservation management therefore engineers a more resilient soil environment that buffers hydrothermal extremes, enhances water-use efficiency, and supports sustainable crop production.

Keywords: ecology, crop rotation, Mollisol, soil moisture sensor, soil structure, tillage.

INTRODUCTION

Soil temperature and moisture regimes are fundamental regulators of soil physical processes, biological activity, and agricultural productivity. In the monsoon-influenced continental climate of Northeast China, characterized by cold, dry winters and warm, humid summers, these factors interact to regulate germination, phenology, nutrient uptake, and yield of the primary row crops, soybean (Glycine max) and maize (*Zea mays*) (Geng et al., 2021; Qi et al., 2022; Jegadeeswari et al., 2025). These seasonal extremes also modulate the timing and intensity of key Mollisol processes, thereby influencing soil fertility and agricultural output (Liu et al., 2016; Mondal, 2021; Bălc et al., 2025; Mammadov et al., 2026). Therefore, understanding the interplay between

soil climate and crop physiology in this region is essential for optimizing management practices and ensuring long-term agricultural resilience under changing environmental conditions (Pikovska, 2020; Dehodyuk et al., 2021; Kravchenko and Bykova, 2023).

The influence of soil temperature extends beyond simple linear scaling of metabolic rate, constituting instead a complex, non-linear control variable that interacts with phenological progression, resource acquisition, and symbiotic associations (Bahuguna and Jagadish, 2015; Onwuka and Mang, 2018; Tsentylo et al., 2019). For maize and soybean, temperature effects are profound and stage-specific, mediated through distinct physiological and morphological pathways (Hatfield and Prueger, 2015; Farahin et al., 2024). Maize, a C_4 species of tropical origin, exhibits a higher base temperature for germination (Tb ≈ 10 °C) compared to soybean (Bonhomme, 2000). Sub-threshold temperatures delay germination, prolong thermal time to emergence, and predispose seedlings to soil-borne pathogens in cool, saturated seedbeds. Post-emergence, suboptimal temperatures suppress coleoptile and mesocotyl elongation, and increase the risk of incomplete stand establishment. Although soybean has a slightly lower Tb (8–10 °C), early-season cold stress constrains nodulation and the establishment of effective symbiosis with Bradyrhizobium japonicum, thereby inducing early nitrogen limitation (Zhang et al., 2001; Yuan et al., 2020; Szczerba et al., 2025). Optimal root elongation for both species occurs between 20–30 °C (Pahlavanian and Silk, 1988). Cold soils (<15 °C) increase cytosolic viscosity, reduce meristematic cell division rates, and promote the development of shallower root systems with reduced lateral branching. This constrains the explorable soil volume, limiting access to water and immobile nutrients. Furthermore, soil temperature directly modulates rhizosphere biogeochemistry by controlling the kinetics of organic matter mineralization, nutrient diffusion, and the activity of root membrane transporters (BassiriRad, 2000; Levine et al., 2023; Pregitzer and King, 2005). Increased viscosity of cold water directly reduces the hydraulic conductivity of both the soil matrix and root tissues. This can induce an isohydric stress, even in matric-moist soils, as root water uptake fails to meet transpiration demand. The concomitant reduction in water flux diminishes the mass-flow delivery of mobile nutrients, compounding nutritional limitations. In temperate continental climates, such as that of Heilongjiang Province, cool spring conditions frequently coincide with high soil moisture. This combination depresses evapotranspiration, promoting profile saturation and the onset of hypoxic or anoxic conditions in the rhizosphere. Cold stress during critical reproductive periods can impair pollen viability, flower abortion rates, and kernel row determination (Miedema, 1982). During grain filling, suboptimal root-zone temperatures reduce the rate and duration of photoassimilate deposition, decreasing individual kernel mass and, in soybean, compromising seed protein synthesis.

For soybean and maize grown in Northeast China, soil moisture exerts distinct controls over biomass production, root system development, nutrient uptake, and reproductive success. Both crops are sensitive to water stress during key reproductive stages (Gaballah et al., 2008; Zhou et al., 2022; Wang et al., 2025). Adequate soil moisture is essential for seed imbibition, enzymatic activation, and uniform emergence. Maize is particularly vulnerable during silking and grain fill, while soybean is most sensitive during flowering and pod set (Wang et al., 2022). Insufficient water during germination delays emergence and reduces stand uniformity, whereas excessive moisture induces hypoxic conditions that suppress respiration and increase susceptibility to soil-borne pathogens (Keska et al., 2021). Maize seedlings are particularly sensitive to early-season waterlogging because of high oxygen demand and limited aerenchyma development (Zhi et al., 2024), whereas soybean shows slightly greater tolerance (Sun et al., 2025) but still exhibits reduced emergence and early vigor under prolonged saturation. Under water deficit, both crops exhibit reduced root elongation rates, although maize often responds by increasing root depth relative to soybean, reflecting its greater reliance on deep soil water during mid-season growth. Maize maintains higher water use efficiency under moderate drought than soybean, but remains highly vulnerable during tasseling and silking (Yu et al., 2004). Although soybean exhibits greater plasticity in vegetative growth, it remains sensitive to water stress during flowering and pod filling, resulting in increased flower abortion and reduced seed size. During rainy periods, persistently wet soils restrict root penetration, reduce root longevity, and impair mycorrhizal associations, limiting access to both water and nutrients (Xu et

al., 2023). Intense monsoon downpours can also lead to transient waterlogging, closing soil pores and creating anaerobic conditions. Maize roots are highly sensitive to oxygen deficiency, while soybean is somewhat more tolerant but suffers from reduced nodulation and nitrogen fixation. The impacts of soil moisture on yield are strongly stage-dependent and crop-specific (Pavlova and Litvinov, 2024). In maize, soil moisture deficits during reproductive stages often result in disproportionate yield losses relative to vegetative stress (Behera et al., 2025). In soybean, yield formation is more evenly sensitive across flowering and seed filling, with cumulative water stress exerting a strong influence on seed number and weight (Zhang et al., 2025).

In intensively managed agroecosystems, temperature and moisture regimes are not only shaped by climate and soil type, but are strongly modified by tillage practices (Wang et al., 2024; Tanchyk et al., 2024). Through tillage effects on residue distribution, aggregate stability, bulk density, and microporosity (Komissarov and Klik, 2020; Kochiieru et al., 2023), it determines how climatic forcing is transmitted into the magnitude and temporal variability of hydro-thermal conditions across the rooting zone. Conventional tillage, which typically incorporates or removes crop residues, increases soil exposure to solar radiation and enhances shortwave absorption, leading to higher daytime soil temperatures and greater diurnal thermal amplitudes in the upper soil layers (O'Brien and Daigh, 2019). A residue-covered surface under conservation tillage tends to buffer thermal fluctuations by increasing albedo compared to plowed soil (Daughtry et al., 2004). No-tilled soils show lower diurnal temperature variation than conventionally tilled soils, often resulting in reduced thermal conductivity (Li et al., 2024). This creates a more insulative surface layer, damping the amplitude and penetration depth of seasonal temperature waves, reducing the vapor pressure gradient driving evaporation. Furthermore, the higher water content under conservation tillage increases volumetric heat capacity, creating stabilizing feedback on the thermal regime. Conservation tillage systems, characterized by continuous macropores and a protected surface structure, typically exhibit elevated saturated hydraulic conductivity. This enhances infiltration, diminishes surface runoff, and encourages preferential flow (Han et al., 2025). In contrast, conventional tillage can seal the surface via raindrop impact, break macropores, reduce hydraulic conductivity, increase runoff and reduce available water capacity by increasing evaporative losses (Liebhard et al., 2022). In general, conservation tillage tends to enhance hydro-thermal stability, while conventional tillage amplifies variability, especially in the near-surface layers.

Understanding the coupled dynamics of soil temperature and moisture is central to interpreting crop performance, soil biological activity, and long-term soil functioning under agricultural management. While the general effects of tillage on soil properties are well-documented in experiments, there is a scarcity of detailed, high-temporal-resolution data on coupled soil temperature and moisture dynamics in soil and subsoil layers under region-specific conditions. The focus on a Mollisol of Northeast China, within its unique monsoon-influenced frigid temperature regime, makes the findings applicable to millions of hectares. This study provides the empirical data needed to parameterize and validate process-based models for this region, moving beyond generic recommendations to predictive understanding. The aim of this study is to quantify and compare the annual dynamics of soil temperature and moisture in a Mollisol under a soybean–maize rotation managed with conventional and conservation tillage systems. Specifically, the study seeks to (i) characterize seasonal and depth-dependent patterns of soil temperature and moisture, and (ii) identify periods of the cropping cycle during which tillage effects on soil hydro-thermal regimes are most evident. Based on this aim, the study tests the following core hypotheses: (1) conservation management moderates soil temperature fluctuations and enhances soil moisture retention relative to conventional tillage in the upper soil layers; (2) differences in soil temperature and moisture between tillage systems are strongest in the surface soil and attenuate with depth; (3) the coupling between soil temperature and moisture will be tillage-specific and season-dependent.

MATERIALS AND METHODS

Experimental site and climatic conditions

The study site was established in 2005 at the Hailun Monitoring and Research Station of the Northeast Institute of Geography and Agroecology, Chinese Academy of Sciences, located on

the outskirts of Hailun City, Heilongjiang Province (47°26′N, 126°38′E). Field observations were conducted from 2010 to 2015. The study area has a monsoon-influenced warm-summer humid continental climate (Köppen *Dwb*) and is characterized by seasonal extremes. The mean annual air temperature is 4.6 °C, with very cold winters (mean January temperature of −18.3 °C) and warm summers (mean July temperature of 23.7 °C). Extreme temperatures range from −33.3 to 37.8 °C. The growing season is short, with 251 days per year with temperatures above 0 °C and 203 days above 5 °C; the accumulated temperature sum above 10 °C (Effective Temperature Sum) is 3234 °C. Annual precipitation averages 553 mm, with 65% occurring between June and August. The mean annual relative humidity is 69%, and total solar radiation is 4.52×10^6 kJ m^{-2} yr^{-1}. A defining feature of the local climate is deep seasonal soil freezing, with maximum frost penetration reaching approximately 195 cm, indicating strong winter thermal control on soil physical and hydrological processes.

According to the Chinese Soil Taxonomy, the Mollisol studied here is classified within the order Isohumosols, the suborder Udic Isohumosols, the group Hapli-Udic Isohumosols, and the subgroup Black soils. Its international equivalents include Haplic Luvic Phaeozems and Haplic Chernozems under the WRB classification (FAO), Udolls in U.S. Soil Taxonomy, and leached moist Chernozems in the Ukrainian classification system (Liu et al., 2011).

At the time of experiment establishment, the Mollisol exhibited the properties presented in Table 1. The soil has a heavy loam texture, with a tendency for the clay fraction to increase by 2.6% in the 70–110 cm layer. In the 0–20 cm layer, the humus content ranges from 4.4 to 4.6 g 100 g^{-1}, which is considered optimal for cultivating agricultural crops (Medvedev, 1997). Below this depth, organic carbon content declines progressively: from 1.4 g 100 g^{-1} in the 30–50 cm layer and 0.5 g 100 g^{-1} in the 90–110 cm layer to 0.2 g 100 g^{-1} in the 150–170 cm layer. The soil exhibits a neutral pH throughout the profile.

Bulk density is optimal for crop growth in the upper 0–10 cm layer (1.11–1.28 g cm^{-3}) and remains within acceptable limits for grain corn and soybean production in deeper horizons. According to the classification of Kachinskii (1965), field capacity is rated as excellent in the 5–50 cm layer (0.464–0.429 cm^3 cm^{-3}) and good in the 0–5, 50–70, and 110–190 cm layers. Saturated water content across the profile ranges from 0.397 to 0.623 cm^3 cm^{-3}, with the highest values observed in the 20–30 cm layer. Its lowest values occur in the deep compacted horizons, where bulk density exceeds 1.5 g cm^{-3} and organic carbon falls below 0.2%. The permanent wilting point (PWP) increases with depth, from 0.117 cm^3 cm^{-3} in the topsoil to a maximum of 0.187 cm^3 cm^{-3} at 170–190 cm. This trend reflects an inverse relationship with the decline in soil organic carbon and a direct relationship with increasing clay content and bulk density in the deeper horizons.

Experimental design

A long-term stationary single-factor experiment was established at the Hailun Monitoring and Research Station in 2005. The experiment was designed as a split-plot system with elementary plots measuring 8.4 × 40 m (336 m²) and control plots of 100 m². For this study, three replicates per treatment were analyzed: no-till (NT), reduced tillage (RT), and conventional tillage (CT) (Figure 1b–d). The studied crop rotation system alternated soybean (2010, 2012, 2014) and maize (2011, 2013, 2015). Both crops were planted with 68–70 cm row spacing, with in-row plant spacing of 25–30 cm for corn and 5 cm for soybeans. Seeds were sown between April 29 and May 6, with harvest occurring from September 28 to October 5. Presowing fertilization (applied at 10 cm depth) included urea, triple superphosphate, and potassium sulfate. Fertilizer was applied at 69.5 kg N ha^{-1}, 51.75 kg P ha^{-1} and 15 kg K ha^{-1} + 100 kg N ha^{-1} (at the seeding stage) for grain corn and 20.25 kg N ha^{-1}, 51.75 kg P ha^{-1} and 15 kg K ha^{-1} for soybeans.

Sampling, measurements and analyses

Annual precipitation and air temperature were recorded at a weather station situated approximately 100 m from the experimental plots (Figure 1 a). The average gravimetric soil water content was measured during the growing seasons (May to September, 2010–2015) at depths of 0–5, 5–10, 10–15, and 15–20 cm. All measurements were taken at the center of the ridge. Undisturbed core samples were collected, sealed in aluminum containers, and transported to the laboratory. Water content was determined by oven-drying at 105 °C to constant mass, following the standard method (Little et al., 1998).

Table 1. Selected physical, physico-chemical, and hydrophysical properties of the Mollisol at the beginning of the scientific experiment, 2004 (Liu et al., 2013)

Soil layer, cm	Soil organic carbon, (g 100 g^{-1})	pH_{H_2O}	Bulk density, g cm^{-3}	Permanent wilting point (cm^3 cm^{-3})	Soil water contents at –0.33 MPa (cm^3 cm^{-3})	Saturated water content (cm^3 cm^{-3})	Silt content (%)	Clay content (%)
0–5	2.7	6.6	1.11	0.117	0.388	0.565	29.3	40.7
5–10	2.7	6.6	1.28	0.144	0.464	0.520	29.3	40.7
10–20	2.6	6.6	1.38	0.148	0.446	0.515	29.3	40.7
20–30	2.1	6.2	1.31	0.148	0.429	0.623	29.6	39.9
30–50	1.4	6.4	1.31	0.153	0.429	0.581	29.1	40.8
50–70	1.0	6.4	1.30	0.136	0.376	0.461	29.1	40.8
70–90	0.9	6.4	1.38	0.130	0.418	0.591	27.9	43.3
90–110	0.5	6.4	1.48	0.165	0.418	0.494	27.9	43.3
110–130	0.4	6.4	1.40	0.168	0.381	0.479	29.9	39.7
130–150	0.3	6.4	1.47	0.176	0.381	0.450	29.9	39.7
150–170	0.2	6.6	1.47	0.176	0.381	0.397	29.9	39.7
170–190	0.1	6.7	1.55	0.187	0.381	0.397	29.9	39.7

Gravimetric water content (θg) was calculated as the mass of water lost divided by the mass of the dry soil solids. Concurrently, soil temperature and volumetric water content (θ_v) at depths of 5, 10, 20, 40, 60, 90, 110, 150, and 270 cm were measured automatically by sensors throughout the year using the complex conductivity method (Liu et al., 2022). Data were stored by a Campbell Scientific CR23X Micrologger® (USA) (Figure 1 e), and weekly average soil temperatures and water content were subsequently calculated.

Statistical analysis

Statistical analyses were performed using Microsoft Excel 2021, IBM SPSS Statistics 20.0 (SPSS Inc., Chicago, IL), and SigmaPlot 14.0 (Systat Software, Inc., 2017). For each measured parameter, we calculated arithmetic means with standard deviations as measures of central tendency and variability. Significant differences among tillage treatments (lowercase superscripts) and among soil layers or sampling dates (uppercase superscripts) were determined using analysis of variance (ANOVA), with p-values adjusted by Bonferroni correction at $\alpha = 0.05$. Statistical significance was accepted at $p < 0.05$. All statistical tests were conducted at a 95% confidence level.

RESULTS

Soil moisture dynamics during the growing season

Soil moisture followed a unimodal seasonal trajectory, with peak values in May, a progressive decline to a minimum in August, and partial autumn recovery (Figure 2). The hierarchy of soil

a b c d e

Figure 1. Hailun monitoring and research station: a – climatic station, b – no-till T plot, c – reduced-till (RT plot, d – convention tillage CT plot, e – Campbell Scientific CR23X Micrologger® (USA)

water content (NT > RT > CT) was statistically significant ($p < 0.001$) across all dates and depths.

The May sampling, conducted following spring thaw and prior to significant crop water demand, revealed a soil profile at high moisture capacity. Despite uniformly high water content, the moisture conservation hierarchy was evident across all depths and positions. The difference was most evident in the surface layer. In the row at 0–5 cm, NT showed a mean moisture content of 22.52 ± 0.60%, which was 1.6 percentage points higher than RT (19.56 ± 1.08%) and

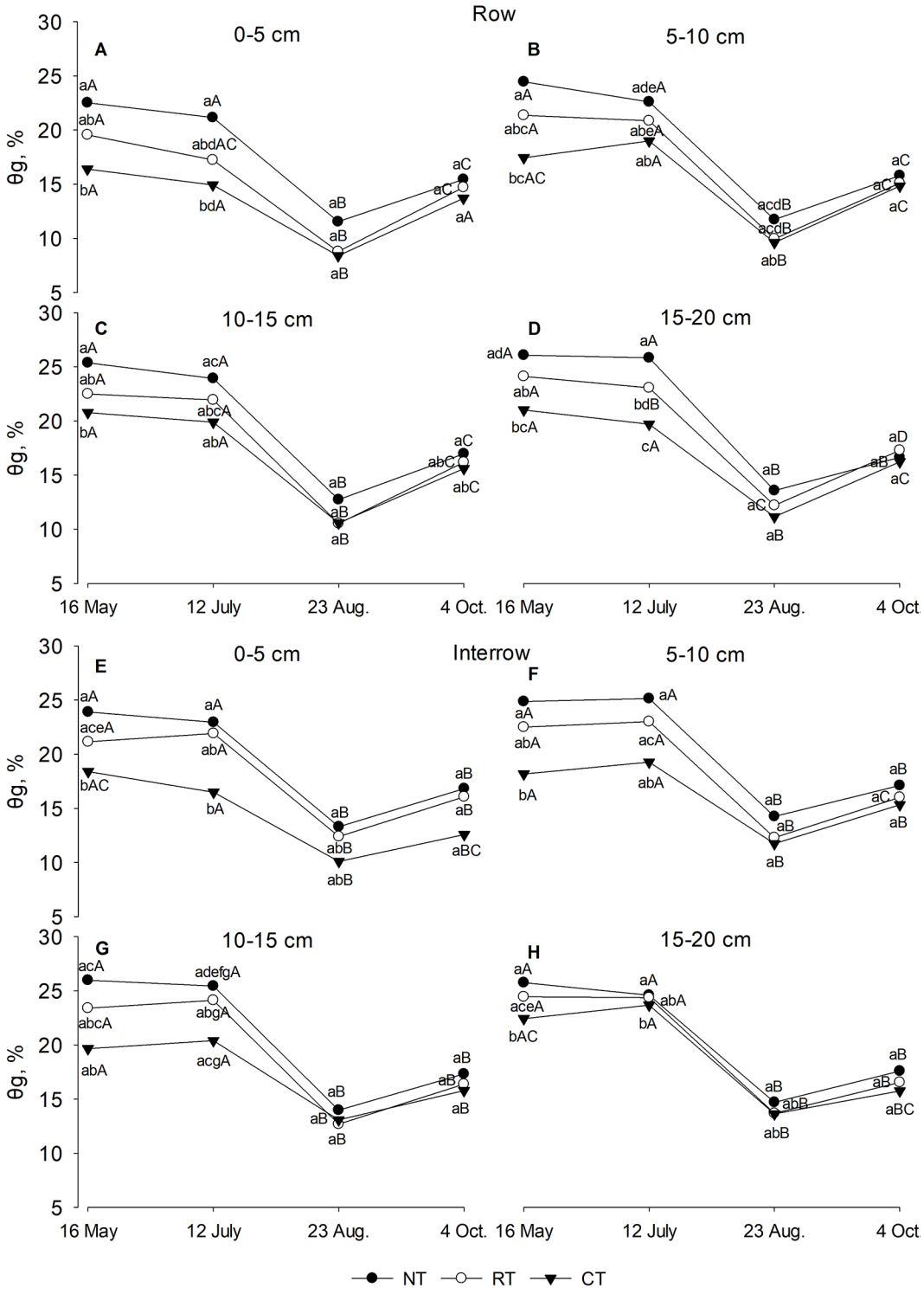

Figure 2. Mean gravimetric water content (θg, %) for 2011-2015 under different tillage systems: NT – no-till, CT– conventional tillage, RT– reduced tillage.
Lowercase letters indicate significant differences among sampling dates (< 0.05)

6.1 percentage points higher (37.3%) than CT (16.40 ± 0.83%). This significant advantage persisted with depth, though the absolute difference narrowed slightly. At 15–20 cm in the row, NT (26.09 ± 0.49%) still held 3.5–4.5% more water content than RT (24.12 ± 0.86%) and CT (21.02 ± 0.68%). Interrow sampling showed slightly higher soil moisture content than in rows. Under NT at 0–5 cm, interrow moisture content was 23.90 ± 0.57%, compared to 22.52 ± 0.60% in the row, a pattern which was repeated across all treatments.

By mid-July, soil moisture content had significantly declined from spring levels across all tillage treatments, depths, and spatial positions. In the row at 0–5 cm, mean moisture content under NT (21.16 ± 0.90%) was 41.7% higher compared to CT (14.93 ± 1.17%), while RT (17.24 ± 1.26%) held an intermediate value. This advantage was consistent across depths. For example, at 15–20 cm in the row, NT retained 25.84 ± 0.17% moisture, compared to 19.71 ± 0.95% under CT. The steepest vertical gradients were observed under NT, where moisture rose from 21.16% at 0–5 cm to 25.84% at 15–20 cm in the row, compared to the more uniformly depleted profile under CT (14.93% to 19.71% over the same interval). Interrow moisture content remained consistently higher than in the row across all treatments.

By late August, soil moisture content reached its seasonal minimum, reflecting the cumulative impact of high evapotranspirative demand and limited summer precipitation. The relative advantage of conservation tillage became stark. In the row at 0–5 cm, NT retained a mean moisture content of 11.55 ± 0.64%, which was 30.7% higher than RT (8.78 ± 0.40%) and 49.4% higher than CT (7.73 ± 1.00%). This substantial advantage held across most depth–spatial positions. For instance, in the interrow at 10–15 cm, NT (13.97 ± 0.42%) accumulated approximately 17% more moisture than CT (11.92 ± 0.87%). The interrow consistently contained substantially higher moisture content than the row across all tillage systems and depths. The difference was most extreme under CT at 0–5 cm, where the interrow (11.10 ± 0.98%) held 43% more water than the row (7.73 ± 1.00%).

By October, soil moisture content had recovered substantially from the late-summer deficit across all treatments. In the row at 0–5 cm, NT contained a mean moisture of 15.45 ± 1.42%, compared to 14.72 ± 0.84% for RT and 13.71 ± 0.86% for CT. The relative differences were most distinct in surface layers. Notably, in the interrow at 0–5 cm, the deficit in CT was more acute: NT (16.82 ± 0.71%) held 33% more moisture than CT (12.64 ± 1.15%), while RT (16.06 ± 0.49%) showed an intermediate value. Soil moisture content generally increased with depth. For example, under NT in the interrow, moisture levels rose from 16.82% (0–5 cm) to 17.59% (15–20 cm). In most cases, interrow moisture content remained slightly higher than in the row for the same tillage and depth.

Soil moisture dynamics during the cold period

Volumetric water content within the 5–270 cm soil profile exhibited complex, non-linear dynamics during the cold period (November–May), reflecting the combined effects of freezing–thawing processes and tillage-induced structural differences Two dominant hydrological phases were identified (Table 2): (1) Autumn–winter freezing phase (November–February): cryogenic moisture redistribution; (2) Spring thaw and rewetting phase (March–May): downward recharge and differential recovery. During the cold phase, the dominant direction of water movement was upward, driven by cryosuction toward the advancing freezing front. The response was strongly stratified by both depth and tillage system. In the surface layers (5–40 cm), all treatments showed moisture accumulation; however, the magnitude differed substantially among systems. CT and RT exhibited drawdowns in volumetric water content (θ_v) exceeding 30–35%, whereas NT displayed a more moderate accumulation (e.g., θ_v at 5 cm of approximately 12–25%). In the mid-depth zone (60–150 cm), CT experienced the most severe drying, with θ_v declining by approximately 15–20 percentage points (e.g., at 150 cm from ~34% to 16.3%). RT showed an intermediate response, while NT demonstrated high moisture stability with minimal winter depletion. At the deepest monitored layer (270 cm), the sensor data revealed a system-scale response.

NT maintained a consistently high and stable θ_v (~37–41%) throughout the freezing period, whereas CT and RT exhibited drawdowns, with θ_v decreasing to 18.2% and 22.1%, respectively. In spring, thawing reversed the hydraulic gradient, directing water predominantly downward via meltwater percolation. In the surface layers (5–40 cm), soil moisture declined as ice melted and evaporation resumed. Surface drying was most rapid under CT, while NT and RT retained moisture for a longer

Table 2. Mean values of volumetric water content (θ_v, %) by depth and tillage system (November–May, 2011–2015)

Depth, cm	Day.Month																		
	09.11.	15.11.	30.11.	15.12.	31.12.	15.1.	31.1.	15.2.	1.3.	15.3.	30.3.	15.4.	28.4.	30.4.	5.5.	10.5.	15.5.	18.5.	23.5.
CT																			
5	7.1	7.3	6.5	6.4	12.8	7.9	9.2	12.5	14.2	17.3	24.6	22.8	20.5	20.7	20.5	26.6	15.7	15.5	14.6
10	15.9	15.2	14.4	15.1	15.2	14.9	15.0	13.4	15.1	15.0	18.5	25.7	26.3	26.1	25.3	25.2	24.7	25.1	21.3
20	25.9	24.8	20.5	19.3	20.0	15.3	18.6	19.0	18.8	18.9	20.9	25.1	33.0	33.1	31.2	32.3	32.7	32.5	32.7
40	31.8	23.2	20.8	21.0	22.4	18.1	19.1	19.4	19.5	19.9	20.5	31.1	31.0	31.3	30.6	30.0	30.8	29.8	29.6
60	32.4	34.7	25.2	22.5	38.5	18.4	22.0	22.0	22.2	21.9	21.8	22.9	32.2	24.2	25.1	32.0	31.1	30.9	22.6
90	35.0	33.9	33.1	34.5	34.6	17.3	25.1	23.3	23.3	23.3	23.2	21.1	25.3	25.5	26.1	28.5	33.4	33.3	20.8
110	34.6	33.9	34.0	33.6	19.4	26.2	25.7	25.2	24.9	24.7	25.0	22.7	24.6	12.0	30.2	26.2	27.0	32.8	32.5
150	34.2	24.6	34.4	35.0	16.3	33.8	33.2	15.8	26.2	26.3	26.3	26.7	15.8	12.6	27.4	27.1	15.9	15.0	22.5
270	35.0	39.5	38.9	38.8	18.2	38.4	38.3	38.6	38.2	38.2	38.2	37.1	37.7	38.3	37.9	32.7	38.3	28.0	31.4
RT																			
5	39.4	21.8	20.2	19.1	20.5	14.6	20.2	19.0	19.6	19.1	23.6	25.5	33.3	27.8	35.7	34.4	33.3	33.9	33.6
10	27.4	22.3	20.7	19.2	25.6	18.3	18.8	18.8	19.3	17.4	21.6	24.2	27.4	33.3	33.1	32.5	32.6	33.2	31.4
20	25.7	26.9	22.1	21.2	22.3	21.4	20.7	21.3	21.9	19.8	20.6	29.9	35.3	36.7	34.5	35.6	33.4	34.1	33.5
40	31.9	20.1	21.4	20.1	19.2	23.9	20.2	20.5	22.8	20.8	21.5	30.1	31.4	27.4	33.3	33.1	22.9	32.5	31.3
60	32.4	32.7	29.4	23.0	27.2	22.2	22.0	21.6	21.5	21.8	22.4	24.1	24.9	25.4	24.7	27.2	32.9	33.2	23.1
90	32.8	33.7	33.3	32.8	31.4	24.6	24.7	24.6	24.5	24.4	24.5	25.6	26.0	28.4	26.3	26.6	15.8	32.8	30.4
110	33.3	32.5	32.6	32.4	18.8	18.4	24.2	24.7	24.5	27.0	24.6	25.2	26.0	31.1	26.5	25.9	27.3	28.3	26.7
150	31.9	37.2	33.8	34.7	20.6	28.5	31.9	17.2	27.1	29.6	25.8	27.3	17.4	33.8	35.7	29.5	17.8	22.7	23.5
270	37.2	27.0	27.7	27.3	22.1	24.6	27.6	28.0	27.6	29.8	27.3	25.8	31.2	36.5	36.9	33.1	35.6	31.6	29.3
NT																			
5	23.8	14.6	12.5	12.2	25.2	14.5	11.4	11.3	11.9	12.4	14.8	19.2	23.7	19.2	22.6	21.9	21.5	20.8	24.1
10	14.6	14.7	12.9	14.2	17.2	13.4	11.8	11.8	12.0	13.0	19.2	23.6	24.6	23.7	27.8	22.0	22.5	22.1	24.9
20	21.2	22.5	18.1	18.6	20.6	16.7	16.8	17.0	17.5	17.2	21.3	31.5	31.4	28.2	33.0	30.9	31.5	30.2	31.7
40	27.2	33.2	22.7	22.1	18.2	21.1	20.8	21.1	20.8	21.2	21.7	23.9	31.9	35.0	33.5	32.0	32.0	32.4	32.6
60	33.8	33.0	26.8	24.1	33.1	23.7	21.7	23.6	23.5	22.9	23.3	24.1	25.3	31.7	29.7	27.3	31.5	32.0	39.1
90	35.6	35.5	35.0	33.7	36.8	25.0	24.0	24.6	24.0	23.5	24.2	29.9	26.8	26.4	37.6	38.9	33.1	30.1	31.5
110	34.3	33.2	34.6	34.3	30.6	26.7	25.0	24.9	25.6	24.1	25.4	26.8	25.7	26.0	30.9	26.5	27.3	27.3	28.9
150	36.8	36.9	37.0	36.3	37.2	36.4	35.2	28.1	26.6	34.7	26.5	26.8	22.8	27.4	31.2	28.0	28.6	34.5	32.5
270	39.6	39.6	40.1	40.4	41.7	40.2	39.5	39.4	39.2	39.6	39.2	38.9	38.9	37.3	39.4	39.1	38.8	39.3	36.1

period. In the intermediate layers (60–150 cm), all systems exhibited increasing θ_v. CT and RT, having experienced greater winter depletion, showed rewetting, whereas NT exhibited more moderate changes due to its higher antecedent moisture status. At 270 cm, θ_v under NT remained high and stable, while CT and RT showed delayed and, in some cases, incomplete recovery by late spring.

Seasonal variability metrics (SD: standard deviation; CV: coefficient of variation, SD/mean × 100; A: amplitude) revealed clear differences in hydrological buffering capacity among tillage systems and along the soil profile (Table 3). In the surface layer (5 cm), variability was greatest under CT (SD = 6.46%; CV = 43.39%) and RT (SD = 7.49%; CV = 28.78%), while NT showed comparatively lower dispersion (SD = 5.10%; CV = 28.71%), indicating reduced short-term sensitivity to atmospheric forcing under residue retention. With increasing depth, variability generally declined, but the rate of attenuation differed markedly among systems. Under CT, SD remained relatively high (≈5–7%) down to 150 cm, and CV exceeded 20% throughout most of the profile, declining below 15% only at 270 cm (CV = 14.58%), suggesting deep penetration of seasonal moisture signals. RT exhibited moderate damping, with SD values decreasing to ~4–5% below 60 cm and CV approaching 15% at 110–270 cm, indicating partial stabilization at intermediate

Table 3. Seasonal statistics of volumetric water content (θ_v, %) by depth and tillage system (November–May, 2011–2015)

Depth (cm)	Mean θ_v (%)	SD* (%)	Amplitude** (%)	CV*** (%)
CT				
5	14.88	6.46	20.20	43.39
10	19.34	5.11	12.90	26.43
20	24.98	6.40	17.80	25.64
40	25.26	5.41	13.70	21.40
60	26.45	5.63	20.10	21.28
90	27.40	5.65	17.70	20.63
110	27.12	5.77	22.60	21.27
150	24.69	7.53	22.40	30.51
270	35.88	5.23	21.30	14.58
RT				
5	26.03	7.49	24.80	28.78
10	25.11	6.02	15.90	23.97
20	27.21	6.40	16.90	23.54
40	25.49	5.40	14.10	21.17
60	25.88	4.25	11.70	16.40
90	27.54	4.58	17.90	16.64
110	26.84	4.22	14.90	15.73
150	27.68	6.38	20.00	23.03
270	29.80	4.35	15.10	14.59
NT				
5	17.77	5.10	13.90	28.71
10	18.21	5.41	16.00	29.72
20	23.99	6.44	16.30	26.84
40	26.49	5.83	16.80	22.01
60	27.91	4.93	17.40	17.68
90	30.33	5.37	15.40	17.70
110	28.32	3.54	10.50	12.51
150	31.76	4.69	14.40	14.76
270	39.28	1.15	5.60	2.92

Note: *SD – standard deviation; **Amplitude – seasonal maximum minus minimum; ***CV – coefficient of variation (SD/mean × 100); NT – no-till, CT – conventional tillage, RT – reduced tillage.

depths. In contrast, NT displayed a reduction in variability beginning at 110 cm (SD = 3.54%; CV = 12.51%), with extremely strong damping at 270 cm (SD = 1.15%; CV = 2.92%). Seasonal amplitude patterns mirrored these trends: CT showed large oscillations at 110 and 150 cm (22.6% and 22.4%), RT exhibited intermediate amplitudes (11.7–20.0%), whereas NT demonstrated substantially lower deep-profile amplitude (5.6% at 270 cm), reflecting strong attenuation of seasonal fluctuations. Overall, SD, amplitude, and CV consistently indicate that no-till management enhances vertical hydraulic damping and reduces seasonal variability at depth, whereas conventional tillage maintains higher oscillatory behavior throughout much of the soil profile.

Annual soil temperature dynamics

Soil temperature exhibited a distinct seasonal wave that transferred downward from the surface, with its amplitude, phase lag, and stability significantly modulated by tillage system and depth (Figure 3). Three thermodynamically discrete phases were identified: autumn cooling, mid-winter stability, and spring warming.

Phase 1 – autumn cooling (November–January): Divergence in thermal inertia. The onset

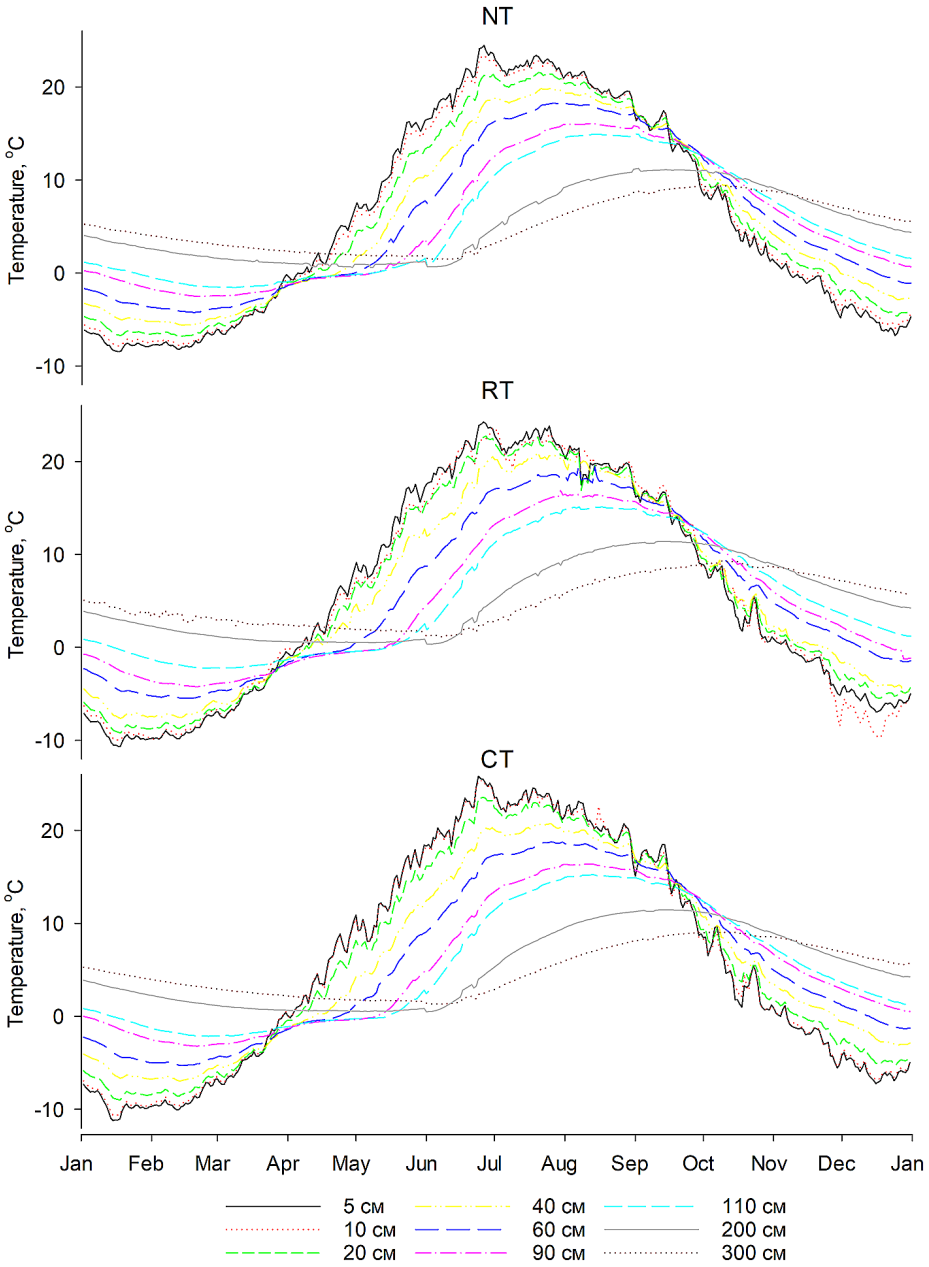

Figure 3. Annual dynamics of Isohumusol temperature under different tillage systems: NT – no-till, CT – conventional tillage, RT – reduced tillage

of surface energy loss initiated a tillage-dependent cooling trajectory. The rate of temperature decline at 5 cm depth was 33% slower under NT (−0.12 °C day^{-1}), compared to CT (−0.18 °C day^{-1}), with RT exhibiting an intermediate rate (−0.15 °C day^{-1}). Consequently, the 0 °C isotherm arrival at 5 cm was delayed by approximately 13 days under NT relative to CT. This delayed cooling propagated with depth; the 0 °C front took 25% longer to reach 20 cm under NT/RT, establishing a significantly colder upper meter (<100 cm) in CT by late January (mean difference: 1.5–2.5 °C). Phase 2 – mid-winter stability (January–February): Latent heat buffering and hydraulic coupling. Peak winter minima revealed a 2.8 °C surface temperature differential between CT (−11.2 °C at 5 cm) and NT (−8.4 °C). The duration of the near-isothermal "zero-curtain" period (temperature at 0 ± 0.5 °C) at 10 cm was prolonged by 108% under NT (25 days) compared to CT (12 days), indicative of extended latent heat release from in-situ ice formation. Deep soil (270 cm) thermal stability was fundamentally altered: NT formed a minimal annual range of ~2 °C, while CT exhibited fluctuations >3 °C. Episodic mid-depth (60–90 cm) warming pulses of +1.0 to +1.5 °C over 48-hour periods were observed

exclusively in CT and RT during January, signaling advective heat transfer via upward water migration. Phase 3 – spring warming (March–May): Asynchronous thaw and energy partitioning. Surface energy partitioning reversed the thermal hierarchy. From March to May, the 5 cm warming rate under CT (+0.25 °C day^{-1}) exceeded NT (+0.17 °C day^{-1}) by 47%, resulting in a 3.1 °C warmer CT surface by mid-May. This differential transmitted downward; by 31 May, the depth of the 10 °C isotherm was ~140 cm in CT versus ~95 cm in NT. Accumulated growing degree days (base 5 °C) at 5 cm from 1 April to 31 May were 420 °C-days for CT compared to 365°C-days for NT, a 13% reduction under conservation management. Thermal hysteresis analysis revealed that for an identical 5 cm temperature in spring, the 20 cm layer remained 1.2–1.8 °C warmer under NT, indicating a legacy heat carry-over from winter latent energy release.

DISCUSSION

The combined soil temperature and moisture datasets demonstrate that the Mollisol responds to climatic forcing not as a stack of independent layers, but as a vertically integrated hydrothermal system whose internal coupling is strongly regulated by tillage-induced structural states. The results support the first two hypotheses, confirming that conservation tillage moderates soil temperature fluctuations and enhances moisture retention, with effects strongest in surface horizons and progressively attenuating with depth. Importantly, the data show that tillage does not merely shift mean thermal or hydraulic conditions, but reorganizes the soil into distinct hydrothermal functional regimes with fundamentally different dynamic responses to seasonal forcing.

Under no-tillage, the soil functions as a high-inertia, capacitively buffered system (Peixoto et al., 2020). The residue-covered surface acts as an effective thermal and hydraulic boundary layer, increasing surface albedo, reducing sensible heat exchange, and suppressing convective mass transfer between the atmosphere and soil (Toshitsugu and Haruhiko, 2002; Thapa and Dura, 2024). This structural configuration explains the slower autumn cooling, the extended winter zero-curtain duration, and the delayed spring warming observed under NT (Dong et al., 2024). Hydrologically, preservation of continuous macropore networks (Blanco-Canqui and Ruis, 2018) and higher infiltration capacity establish a consistent NT > RT > CT moisture hierarchy throughout much of the profile. Elevated volumetric water content increases soil heat capacity, reinforcing thermal damping through a positive feedback between moisture retention and temperature stability (Barreiro et al., 2020; Kovalchuk, 2021). The exceptional thermal stability observed at 270 cm depth, where NT exhibited a temperature range of only ~2 °C, indicates effective decoupling of deep soil processes from surface climatic extremes. This deep buffering is critical for sustaining subsoil biological activity and limiting temperature-driven carbon losses (Possinger et al., 2021; Haque et al., 2024). In contrast, conventional tillage operates as a conductively dominated hydrothermal system (Al-Shammary et al., 2025). Peng et al. (2023) demonstrated that mechanical disturbance and residue removal increase surface thermal admittance, facilitating rapid heat exchange and deeper penetration of thermal signals (O'Brien and Daigh, 2019). This is reflected in enhanced winter cold propagation, episodic mid-winter warming events, and accelerated spring warming (Parkin et al., 2013). Hydrologically, surface sealing and disruption of structural continuity under CT reduce infiltration and increase evaporative losses (Arshad et al., 1999), as evidenced by surface drying during mid- to late summer (Tanchyk et al., 2021). Reduced soil moisture lowers volumetric heat capacity, amplifying temperature variability and reinforcing a destabilizing feedback between drying and thermal extremes. The deeper penetration of the 10 °C isotherm in spring under CT relative to NT further indicates stronger vertical thermal connectivity and reduced buffering capacity. Reduced tillage consistently exhibited intermediate behavior but frequently converged toward CT, particularly with respect to deep-profile thermal variability and winter moisture depletion at 270 cm. This suggests the existence of a tillage-intensity threshold, beyond which even intermittent disturbance compromises the structural coherence required to maintain deep hydraulic connectivity and long-term buffering. These contrasting tillage-specific regimes directly address the third hypothesis. Under NT, soil temperature and moisture are coupled through stabilizing feedbacks: higher moisture increases heat capacity, dampening thermal fluctuations, which limits evaporative losses and preserves water availability. This pattern is also observed

in other soils, such as Fluventic Xerochrept and Lithic Xeric Torriorthent (Lampurlanés and Cantero-Martínez, 2006). Under CT, the coupling is predominantly destabilizing: lower moisture reduces heat capacity, enhancing thermal variability, which accelerates evaporation and further depletes soil water, particularly during summer. Consequently, soil temperature and moisture cannot be interpreted independently; their co-variation defines the effective energy–water regime governing root-zone conditions, microbial activity, and plant stress responses.

Strong seasonal hysteresis in temperature–moisture relationships further emphasizes the importance of temporal context. During early spring, CT exhibited a clear thermal advantage, accumulating approximately 55 °C GDD_5 (cumulative growing degree days at 5 °C) more than NT at 5 cm depth by late May. This thermal gain could advance maize emergence given its higher base temperature (Tb) requirement (≈10 °C). However, this benefit coincided with substantially lower surface moisture, with CT retaining only ~60% of NT θ_v values. For soybean, which has a slightly lower base temperature but a strong dependence on soil moisture for Bradyrhizobium mobility and root infection (Szczerba et al., 2025), the hydraulically stable environment under NT may outweigh the thermal delay. This illustrates a central agronomic trade-off: systems optimized for early thermal accumulation may incur hydraulic constraints, whereas systems optimized for moisture retention may delay early phenology. During the summer moisture deficit period, the moisture hierarchy intensified, with NT maintaining up to 50% higher surface θ_v than CT, while temperature differences among treatments were minimal. At this stage, water availability rather than temperature became the dominant limiting factor for both maize (silking) and soybean (pod set). Higher soil water potential under NT supports higher leaf water potential, sustaining turgor-driven growth processes and delaying stomatal closure under atmospheric demand. In contrast, row–interrow moisture gradients under CT indicate spatially heterogeneous water availability, increasing localized stress and reducing overall water-use efficiency. Cold-season dynamics emerged as a critical preparatory phase rather than a dormant interval. Under NT, retention of water in situ and formation of a shallower, thermally buffered frost front preserved both liquid water and hydraulic connectivity. This minimized cryogenic disruption and prevented the deep-water mining observed under CT, where upward cryosuction concentrated water near the freezing front at the expense of subsoil reserves. As a result, NT entered spring with a larger and more accessible soil water reservoir and potentially greater availability of mobile nitrogen derived from overwinter mineralization (Li et al., 2023). In contrast, CT exported deep water into transient ice lenses, creating a hydrologic deficit that relied on spring precipitation for recovery.

These hydrothermal regimes have cascading implications for soil biogeochemistry and long-term system resilience. Warmer winter soils under NT may enhance heterotrophic respiration, but this effect is likely moderated by physical protection of organic matter within stable aggregates and by higher, more consistent moisture conditions that favor microbial efficiency over biomass turnover (Sadiq et al., 2024). Conversely, CT-induced structural disruption and greater thermal variability may promote pulsed mineralization and increased gaseous losses, reducing carbon-use efficiency. The prolonged zero-curtain and episodic unfrozen water availability under NT create extended biogeochemical "hot moments" for microbial nitrogen transformations, potentially increasing overwinter denitrification risk while moderating the magnitude of spring nitrogen immobilization. Under CT, advective upward transport during freezing may concentrate soluble nitrogen near the surface, increasing vulnerability to runoff losses during snowmelt.

Overall, the buffering capacity inherent to the NT regime represents a key climate-adaptive trait. Enhanced infiltration reduces flood risk, moderated thermal regimes buffer against heatwaves and cold snaps, and conserved deep soil water improves drought resilience. This represents a comparatively high-stability management regime. In contrast, CT represents a low-stability regime, increasing susceptibility to both waterlogging and drought. Under projected climate scenarios characterized by warmer winters and more intense precipitation events, the structural integrity and hydrological decoupling associated with NT are likely to confer increasing agronomic and environmental advantages, although they may necessitate complementary agronomic adjustments.

This study provides a mechanistic framework for identifying distinct soil physical

functional states that can be used to predict management outcomes. The capacitive–buffered regime under no-tillage and the conductive–advective regime under conventional tillage emerge not as descriptive metaphors, but as predictable consequences of tillage-induced changes in thermal and hydraulic connectivity. Conservation tillage fundamentally reconfigures the hydrothermal functioning of Mollisols, not merely at the surface but across the entire soil profile. By reducing vertical energy and water fluxes associated with structural disruption, NT limits resource losses while enhancing profile-scale coherence. In cold-region agroecosystems, where freeze–thaw processes and seasonal water redistribution dominate soil behavior, these structural controls are particularly consequential. The capacity of NT to dampen thermal extremes, conserve deep soil water, and preserve intermediate-layer buffering defines a clear structural pathway through which conservation tillage enhances long-term soil functioning and increases the resilience of crop production systems under variable climatic forcing.

CONCLUSIONS

This research provides a comprehensive, high-resolution elucidation of how tillage fundamentally reconfigures the coupled hydrothermal regime of Mollisols in a seasonally frozen, monsoon-influenced climate under a soybean–maize rotation in Northeast China. The interaction between soil temperature and moisture was shown to be strongly tillage- and season-specific. Rather than merely modifying individual soil parameters, long-term tillage practices established two distinct, self-reinforcing pedophysical regimes: a capacitive-buffered regime under no-tillage and a conductive-advective regime under conventional tillage.

The no-tillage regime, characterized by a high degree of structural complexity, prioritizes conservation and system stability. Enhanced infiltration and reduced evaporative losses promote superior moisture retention, establishing a stabilizing feedback whereby elevated water content increases soil thermal inertia and buffers against temperature extremes. No-tillage consistently exhibited dampened thermal amplitudes, effectively decoupling deep soil layers from surface climatic forcing, conserving subsoil water during freeze–thaw cycles, and maintaining more stable root-zone conditions during periods of peak evaporative demand. These properties produce a delayed yet resilient seasonal trajectory, expressed as slower autumn cooling, a prolonged zero-curtain period sustained by latent heat release, and attenuated spring warming. Critically, NT enters the growing season with a conserved deep soil water reservoir and maintains up to 49% higher surface moisture during summer, directly supporting crop water availability during the most sensitive reproductive stages of both maize and soybean.

Conversely, the conventional tillage regime, defined by structural simplification and surface exposure, is characterized by rapid transmission of thermal signals, strong seasonal temperature gradients, and pronounced moisture depletion, particularly during winter cryogenic redistribution and summer drought. Reduced volumetric water content under CT lowers soil heat capacity, amplifying temperature variability and enhancing conductive and advective heat transfer, thereby reinforcing destabilizing feedbacks between soil drying and thermal extremes. These processes accelerate seasonal transitions, promote deeper winter freezing, and induce substantial depletion of deep soil water through upward cryosuction toward the freezing front. Although CT provides a measurable spring thermal advantage accumulating approximately 55 additional growing degree days (>5 °C) by late May, this benefit is fundamentally offset by its intrinsic hydrological vulnerability and the legacy effects of wintertime resource redistribution.

Overall, this study reframes the core agronomic trade-off not as a simple choice between ‘warm’ or ‘wet’ soils, but as a strategic decision between short-term thermal opportunity and long-term hydrological assurance. In this climate-vulnerable region, the resilience conferred by the NT regime, through its capacity to buffer thermal extremes, conserve deep soil water, and enhance water-use efficiency, represents a more robust and future-proof foundation for sustainable production. Future research should focus on integrating these mechanistic insights into predictive crop models and breeding strategies to fully exploit conservation-based management. Collectively, these findings position no-tillage as a foundational management strategy for engineering climate-resilient soil systems across temperate Mollisol agroecosystems.

REFERENCES

1. Al-Shammary, A., Al-Shihmani, L., Fernández-Gálvez, J., Caballero-Calvo, A. (2025). A comprehensive review of impacts of soil management practices and climate adaptation strategies on soil thermal conductivity in agricultural soils. *Reviews in Environmental Science and Biotechnology, 24*, 513–543. https://doi.org/10.1007/s11157-025-09730-w
2. Arshad, M. A., Franzluebbers, A. J., Azooz, R. H. (1999). Components of surface soil structure under conventional and no-tillage in northwestern Canada. *Soil and Tillage Research, 53*(1), 41–47. https://doi.org/10.1016/S0167-1987(99)00075-6
3. Bahuguna, R., Jagadish, K. (2015). Temperature regulation of plant phenological development. *Environmental and Experimental Botany, 111*, 83–90. https://doi.org/10.1016/j.envexpbot.2014.10.007
4. Bălc, R., Gligor, D., Roba, C., Dicu, T., Rosian, G., Mico, L. (2025). Influence of crop phenology and seasonality on soil conditions across depth profiles. *Crops, 5*, 67. https://doi.org/10.3390/crops5050067
5. Barreiro, A., Lombao, A., Martín, A., Cancelo-González, J., Carballas, T., Díaz-Raviña, M. (2020). Soil heating at high temperatures and different water content: Effects on soil microorganisms. *Geosciences, 10*(9), 355. https://doi.org/10.3390/geosciences10090355
6. BassiriRad, H. (2000). Kinetics of nutrient uptake by roots: Responses to global change. *New Phytologist, 147*(1), 155–169. https://doi.org/10.1046/j.1469-8137.2000.00682.x
7. Behera, S., Kar, I., Yadav, A., Sahu, A. (2025). Exploring waterlogging challenges, causes and mitigating strategies in maize (*Zea mays* L.). *Journal of Agronomy and Crop Science, 211*(5), e70109. https://doi.org/10.1111/jac.70109
8. Blanco-Canqui, H., Ruis, S. (2018). No-tillage and soil physical environment. *Geoderma, 326*, 164–200. https://doi.org/10.1016/j.geoderma.2018.03.011
9. Bonhomme, R. (2000). Bases and limits to using "degree-day" units. *European Journal of Agronomy, 13*(1), 1–10. https://doi.org/10.1016/S1161-0301(00)00058-7
10. Daughtry, C., Hunt, E., McMurtrey, J. (2004). Assessing crop residue cover using shortwave infrared reflectance. *Remote Sensing of Environment, 90*(1), 126–134. https://doi.org/10.1016/j.rse.2003.10.023
11. Dehodyuk, E., Dehodyuk, S., Borko, Y., Litvinova, O., Ihnatenko, Y., Mulyarchuk, A. (2021). Long-term monitoring of aridization in agriculture under climate change in Ukraine. *Plant and Soil Science, 12*(4), 102–114. https://doi.org/10.31548/agr2021.04.102
12. Dong, Z., Yang, S., Li, S., Fan, P., Wu, J., Liu, Y., Wang, X., Zhang, J., Zhai, C. (2024). Effects of no-tillage on field microclimate and yield of winter wheat. *Agronomy, 14*(12), 3075. https://doi.org/10.3390/agronomy14123075
13. Farahin, S., Patah, A., Othman, T., Maizatul, D., Othman, I. (2024). Influence of soil temperature on root development and microbial diversity in paddy fields: A comprehensive review. *Trends in Ecology & Evolution, 2*, 1–9. https://doi.org/10.62622/teiee.024.2.4.01-09
14. Gaballah, M., Ouda, S., Khalil, F. (2008). Effect of water stress on the yield of soybean and maize grown under different intercropping patterns. In *Twelfth International Water Technology Conference (IWTC12 2008)* (pp. 611–624). Alexandria, Egypt.
15. Geng, M., Zhang, F., Chang, X., Wu, Q., Liang, L. (2021). Spatial-temporal variation of soil moisture in China from long time series based on GLDAS-Noah. *Sensors and Materials, 33*(12), 4643–4658. https://doi.org/10.18494/SAM.2021.3445
16. Han, J., Li, J., Chen, Q., Zhang, X. (2025). Long-term conservation tillage breaks the plough pan and promotes the development of preferential flow. *Geoderma, 458*, 117329. https://doi.org/10.1016/j.geoderma.2025.117329
17. Haque, M., Ku, S., Haruna, S. (2024). Soil thermal properties: Influence of no-till cover crops. *Canadian Journal of Soil Science, 104*(3), 246–256. https://doi.org/10.1139/cjss-2023-0095
18. Hatfield, J. L., Prueger, J. H. (2015). Temperature extremes: Effect on plant growth and development. *Weather and Climate Extremes, 10*, 4–10. https://doi.org/10.1016/j.wace.2015.08.001
19. Jegadeeswari, D., Dheebakaran, G., Meena, M., Panchulakshmi, M., Kokilavani, S. (2025). Soil temperature dynamics and their implications for soil health and crop productivity: A critical review. *Plant Science Today, 12*(sp4). https://doi.org/10.14719/pst.10057
20. Kachinskii, N. A. (1965). *Soil physics* (Vol. 1). Vysshaia Shkola. (In Russian).
21. Keska, K., Szczesniak, M., Makałowska, I., Czernicka, M. (2021). Long-term waterlogging as a factor contributing to hypoxia stress tolerance enhancement in cucumber: Comparative transcriptome analysis of waterlogging-sensitive and tolerant accessions. *Genes, 12*, 189. https://doi.org/10.3390/genes12020189
22. Kochiieru, M., Feiza, V., Feiziene, D., Lamorski, K., Deveikyte, I., Seibutis, V., Pranaitiene, S. (2023). Long-term contrasting tillage in

Cambisol: Effect on water-stable aggregates, macropore network and soil chemical properties. *International Agrophysics, 37*(1), 59–67. https://doi.org/10.31545/intagr/156632

23. Komissarov, M., Klik, A. (2020). The impact of no-till, conservation, and conventional tillage systems on erosion and soil properties in Lower Austria. *Eurasian Soil Science, 53*, 503–511. https://doi.org/10.1134/S1064229320040079
24. Kovalchuk, V. (2021). The method of obtaining soil water-physical properties via their granulometric composition. *Plant and Soil Science, 12*(4), 115–125. https://doi.org/10.31548/agr2021.04.115
25. Kravchenko, Y., Bykova, O. (2023). Physicochemical and agrochemical indicators of typical chernozem and isohumisol under various tillage and fertiliser systems. *Plant and Soil Science, 14*(1), 22–38. https://doi.org/10.31548/plant1.2023.22
26. Lampurlanés, J., Cantero-Martínez, C. (2006). Hydraulic conductivity, residue cover and soil surface roughness under different tillage systems in semiarid conditions. *Soil and Tillage Research, 85*(1–2), 13–26. https://doi.org/10.1016/j.still.2004.11.006
27. Levine, C. P., Hayashi, S., Ohmori, Y., Kusano, M., Kobayashi, M., Nishizawa, T., Kurimoto, I., Kawabata, S., Yamori, W. (2023). Controlling root zone temperature improves plant growth and pigments in hydroponic lettuce. *Annals of Botany, 132*(3), 455–470. https://doi.org/10.1093/aob/mcad127
28. Li, H., Liu, P., Zhang, H., Liu, X., Chang, L., Sun, W. (2024). Corn straw mulching mechanized no-tillage approach optimizes farmland soil temperature to increase potato yield in regions of northwestern China. *Agronomy, 14*(11), 2483. https://doi.org/10.3390/agronomy14112483
29. Li, J., Hu, W., Chau, H., Beare, M., Cichota, R., Teixeira, E., Moore, T., Di, H., Cameron, K., Guo, J., Xu, L. (2023). Response of nitrate leaching to no-tillage is dependent on soil, climate, and management factors: A global meta-analysis. *Global Change Biology, 29*, 2172–2187. https://doi.org/10.1111/gcb.16618
30. Liebhard, G., Klik, A., Neugschwandtner, R., Nolz, R. (2022). Effects of tillage systems on soil water distribution, crop development, and evaporation and transpiration rates of soybean. *Agricultural Water Management, 269*, 107719. https://doi.org/10.1016/j.agwat.2022.107719
31. Little, K. M., Metelerkamp, B., Smith, C. W. (1998). A comparison of three methods of soil water content determination. *South African Journal of Plant and Soil, 15*(2), 80–89. https://doi.org/10.1080/02571862.1998.10635121
32. Liu, S., Li, J., Zhang, X. (2022). Simulations of soil water and heat processes for no tillage and conventional tillage systems in Mollisols of China. *Land, 11*(3), 417. https://doi.org/10.3390/land11030417
33. Liu, S., Yang, J., Zhang, X., Drury, C., Reynolds, W., Hoogenboom, G. (2013). Modelling crop yield, soil water content and soil temperature for a soybean–maize rotation under conventional and conservation tillage systems in Northeast China. *Agricultural Water Management, 123*, 32–44. https://doi.org/10.1016/j.agwat.2013.03.001
34. Liu, X., Burras, L., Kravchenko, Y., Duran, A., Huffman, T., Morrás, H., Studdert, G., Zhang, X., Cruse, R., Yuan, X. (2011). Overview of Mollisols in the world: Distribution, land use and management. *Canadian Journal of Soil Science, 92*, 383–402. https://doi.org/10.4141/cjss2010-058
35. Liu, Y., Lei, W., Liu, B., Henderson, M. (2016). Observed changes in shallow soil temperatures in Northeast China, 1960–2007. *Climate Research, 67*, 31–42. https://doi.org/10.3354/cr01351
36. Mammadov, G. S., Teymurov, M. A., Mammadov, Z. R., Yusifova, M. M., Osmanova, S. A., Gasimov, A. M., Akhundova, A. A., Salimova, S. J. (2026). Climate change effects on soil fertility and moisture in the Nakhchivanchay River Basin, Azerbaijan. *International Journal of Agriculture and Biosciences, 15*(1), 77–86. https://doi.org/10.47278/journal.ijab/2025.15
37. Medvedev, V. V. (Ed.). (1997). *Agroecological evaluation of Ukrainian lands and crop placement*. Agrarnaia Nauka. (In Russian).
38. Miedema, P. (1982). The effects of low temperature on *Zea mays*. *Advances in Agronomy, 35*, 93–128. https://doi.org/10.1016/S0065-2113(08)60322-3
39. Mondal, S. (2021). Impact of climate change on soil fertility. In D. K. Choudhary, A. Mishra, & A. Varma (Eds.), *Climate change and the microbiome* (Soil Biology, Vol. 63). Springer. https://doi.org/10.1007/978-3-030-76863-8_28
40. O'Brien, P., Daigh, A. (2019). Tillage practices alter the surface energy balance: A review. *Soil and Tillage Research, 195*, 104354. https://doi.org/10.1016/j.still.2019.104354
41. Onwuka, B., Mang, B. (2018). Effects of soil temperature on some soil properties and plant growth. *Advances in Plants & Agriculture Research, 8*(1), 34–37. https://doi.org/10.15406/apar.2018.08.00288
42. Pahlavanian, A. M., Silk, W. K. (1988). Effect of temperature on spatial and temporal aspects of growth in the primary maize root. *Plant Physiology, 87*(2), 529–532. https://doi.org/10.1104/pp.87.2.529

43. Parkin, G., von Bertoldi, A. P., McCoy, A. J. (2013). Effect of tillage on soil water content and temperature under freeze–thaw conditions. *Vadose Zone Journal, 12*, vzj2012.0075. https://doi.org/10.2136/vzj2012.0075
44. Pavlova, Y., Litvinov, D. (2024). The influence of previous crops and tillage on available moisture reserves of typical chernozem for growing spring barley. *Plant and Soil Science, 15*(2), 32–41. https://doi.org/10.31548/plant2.2024.32
45. Peixoto, D., da Silva, L., Melo, L., Azevedo, R., Araújo, B., de Carvalho, T., Moreira, S., Curi, N., Silva, B. (2020). Occasional tillage in no-tillage systems: A global meta-analysis. *Science of the Total Environment, 745*, 140887. https://doi.org/10.1016/j.scitotenv.2020.140887
46. Peng, Q., Liu, B., Hu, Y., Wang, A., Guo, Q., Yin, B., Cao, Q., He, L. (2023). The role of conventional tillage in agricultural soil erosion. *Agriculture, Ecosystems & Environment, 348*, 108407. https://doi.org/10.1016/j.agee.2023.108407
47. Pikovska, O. (2020). Conservation of fertility of ordinary chernozem under climate aridization conditions. *Plant and Soil Science, 11*(1), 62–68. https://doi.org/10.31548/agr2020.01.062
48. Possinger, A., Weiglein, T., Bowman, M., Gallo, A., Hatten, J., Heckman, K., Matosziuk, L., Nave, L., Sanclements, M., Swanston, C., Strahm, B. (2021). Climate effects on subsoil carbon loss mediated by soil chemistry. *Environmental Science & Technology, 55*(23), 16224–16235. https://doi.org/10.1021/acs.est.1c04909
49. Pregitzer, K., King, J. (2005). Effects of soil temperature on nutrient uptake. In H. Bassiri-Rad (Ed.), *Nutrient acquisition by plants* (Ecological Studies, Vol. 181). Springer. https://doi.org/10.1007/3-540-27675-0_10
50. Qi, W., Feng, L., Yang, H., Liu, J. (2022). Warming winter, drying spring and shifting hydrological regimes in Northeast China under climate change. *Journal of Hydrology, 606*, 127390. https://doi.org/10.1016/j.jhydrol.2021.127390
51. Sadiq, M., Rahim, N., Tahir, M. M., Alasmari, A., Alqahtani, M. M., Albogami, A., Ghanem, K. Z., Abdein, M. A., Ali, M., Mehmood, N., Yuan, J., Shaheen, A., Shehzad, M., El-Sayed, M. H., Chen, G., Li, G. (2024). Conservation tillage: A way to improve yield and soil properties and decrease global warming potential in spring wheat agroecosystems. *Frontiers in Microbiology, 15*, 1356426. https://doi.org/10.3389/fmicb.2024.1356426
52. Sun, Y., Chen, L., Jin, Y., Wang, S., Ma, S., Yu, L., Tang, C., Ye, Y., Li, M., Zhou, W., Chen, E., Kong, X., Fu, J., Wang, J., Chen, Q., Yang, M. (2025). Identification of key waterlogging-tolerance genes in cultivated and wild soybeans via integrated QTL–transcriptome analysis. *Agronomy, 15*(8), 1916. https://doi.org/10.3390/agronomy15081916
53. Szczerba, A., Płażek, A., Kopeć, P. (2025). Mitigating soil drought effects in soybean with *Bradyrhizobium japonicum* inoculants. *BMC Plant Biology, 25*, 1533. https://doi.org/10.1186/s12870-025-07571-x
54. Tanchyk, S., Dudka, O., Pavlov, O., Babenko, A. (2021). Influence of farming systems and soil tillage on available moisture stocks of typical black soil in spring wheat crops. *Plant and Soil Science, 12*(3), 38–47. https://doi.org/10.31548/agr2021.03.038
55. Tanchyk, S., Pavlov, O., Babenko, A. (2024). Theoretical substantiation and development of ecologically friendly farming system in Ukraine. *Plant and Soil Science, 15*(2), 55–66. https://doi.org/10.31548/plant2.2024.55
56. Thapa, B., Dura, R. (2024). A review on tillage system and no-till agriculture and its impact on soil health. *Archives of Agriculture and Environmental Science, 9*(3), 612–617. https://doi.org/10.26832/24566632.2024.0903028
57. Toshitsugu, M., Haruhiko, H. (2002). The effects of tillage on soil temperature and soil water. *Soil Science, 167*, 548–559. https://doi.org/10.1097/00010694-200208000-00006
58. Tsentylo, L., Tsyuk, O., Melnyk, V. (2019). Energy efficiency of growth, transport and processing systems. *Biological Resources and Nature Management, 11*(3–4), 90–96. https://doi.org/10.31548/bio2019.03.010
59. Wang, C., Ai, S., Chen, Q., Li, J., Ding, J., Yang, F. (2024). Effect of strip tillage widths on soil moisture, soil temperature and soil structure in Northeast China. *Frontiers in Environmental Science, 12*, 1404971. https://doi.org/10.3389/fenvs.2024.1404971
60. Wang, X., Cheng, Z., Cheng, X., Wang, Q. (2022). Effects of surface mulching on the growth and water consumption of maize. *Agriculture, 12*, 1868. https://doi.org/10.3390/agriculture12111868
61. Wang, Z., Yu, Y., Chen, X., Li, Y., Jones, A., Rose, R., Ruan, Y., Song, Y. (2025). Mitigating drought-associated reproductive failure in maize: From physiological mechanisms to practical solutions. *The Crop Journal, 13*(4), 1022–1031. https://doi.org/10.1016/j.cj.2025.05.004
62. Xu, F.-L., Hu, P.-M., Wan, X., Harrison, M. T., Liu, K., Xiong, Q.-X. (2023). Crop sensitivity to waterlogging mediated by soil temperature and growth stage. *Frontiers in Plant Science, 14*, 1262001. https://doi.org/10.3389/fpls.2023.1262001
63. Yu, G., Wang, Q., Zhuang, J. (2004). Modeling the water use efficiency of soybean and maize plants under environmental stresses: Application of a synthetic model of photosynthesis–transpiration

based on stomatal behavior. *Journal of Plant Physiology, 161*(3), 303–318. https://doi.org/10.1078/0176-1617-00972

64. Yuan, K., Reckling, M., Ramirez, M. D. A., Djedidi, S., Fukuhara, I., Ohyama, T., Yokoyama, T., Bellingrath-Kimura, S. D., Halwani, M., Egamberdieva, D., Ohkama-Ohtsu, N. (2020). Characterization of rhizobia for the improvement of soybean cultivation under cold conditions in Central Europe. *Microbes and Environments, 35*(1), ME19124. https://doi.org/10.1264/jsme2.ME19124
65. Zhang, L., Wang, R., Hesketh, J. D. (2001). Effects of photoperiod on growth and development of soybean floral bud in different maturity groups. *Agronomy Journal, 93*(4), 944–948. https://doi.org/10.2134/agronj2001.934944x
66. Zhang, Y., Chen, X., Geng, S., Zhang, X. (2025). A review of soil waterlogging impacts, mechanisms, and adaptive strategies. *Frontiers in Plant Science, 16*, 1545912. https://doi.org/10.3389/fpls.2025.1545912
67. Zhi, F., Zhang, J., Bao, Y., Bao, Y., Dong, Z., Tong, Z., Liu, X. (2024). Assessment of waterlogging hazard during maize growth stage in the Songliao Plain based on daily scale SPEI and SMAI. *Agricultural Water Management, 304*, 109081. https://doi.org/10.1016/j.agwat.2024.109081
68. Zhou, Q., Song, S., Wang, X., Yan, C., Ma, C., Dong, S. (2022). Effects of drought stress on flowering soybean physiology under different soil conditions. *Plant, Soil and Environment, 68*(10), 487–498. https://doi.org/10.17221/237/2022-PSE